Chapter 4

Simulation and experimental description

The whole sliding mode estimator design is divided into two parts. One is software simulation, using Matlab®–Simulink®. The other is a hardware experiment verified by using PC-based control system. The whole system description and block diagram will be proposed in section 4.1, followed by hardware experiment presented in section 4.2.

4.1 System Descriptions and Block Diagram

In general, the PMAC motor drive system consists of three components: PWM generator, driver circuit and control algorithm embedded with inner and outer circles. Specifically, the inner circle is current feedback control; the outer speed feedback control. The PMAC motor drive system will be shown in Figure 4.1.

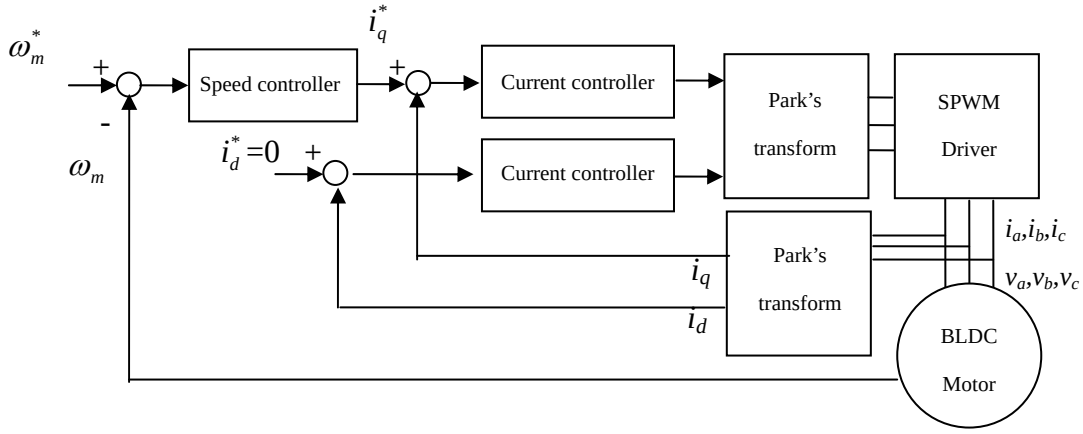

Figure. 4.1 The PMAC motor drive system.

In fact, the control method designed in rotating reference frame is called field-oriented control (FOC). FOC is sometimes called vector control, implying that a current vector should be controlled rather than being only one current component, as in the case of a DC motor. For the inner current feedback control, the reference current i_{qs}^{*} determined from the speed controller is used to control the motor acceleration and deceleration; the reference current i_{ds}^{*} is normally set to zero so that the motor is able to provide a constant torque. For the outer speed feedback control loop, most control techniques may be applied, with the exception of high gain and sliding mode techniques, since the reference input of the inner current control loop should have bounded time derivative. Through the current controller, two new rotating reference frame voltage commands v_{ds}^{*} and v_{qs}^{*} are obtained immediately and put into motor driver.

However, there are two difficulties in obtaining i_{ds} and i_{qs}. One is due to the noise in the measured phase currents; the other is the coordinate transformation. The noise problem is inevitable, whereas the second difficulty lies in the speed limitation of the calculation unit used for transformation. Usually, the phase currents are high frequency signals compared to the i_{ds} and i_{qs}. These high frequency signals must be sampled with a high enough sampling rate, otherwise information will be lost.

Therefore, the sliding mode estimator presented in section 3.3 will be added

upon the outer loop and ignore the inner loop. The difference between sensorless control method and FOC is motor speed calculated from estimators without speed transducer and the output of PID controller control the hysteresis PWM current. The whole sensorless control block diagram is shown in Figure 4.2.

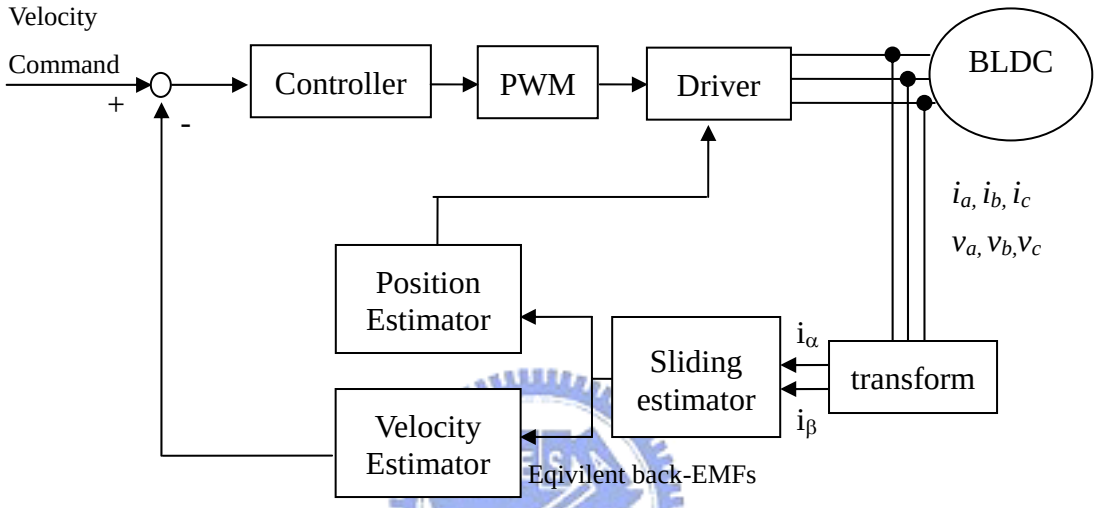

Figure. 4.2 The block diagram of the sensorless speed control

Hence, a trapezoidal BLDC motor is modeled by using the Stateflow® toolbox, a useful toolbox in Matlab®–Simulink®. The Stateflow® toolbox is a visual design and development tool. In addition, the Stateflow® toolbox programs are all written in a dichotomy method so the model is easy to implement. The modeling of the BLDC motor is composed of three parts: three phase back_EMFs, voltages, and hysteresis PWM currents. The explanation of the design process will be depicted as follows.

The ideal trapezoidal back-EMFs and torque production of the BLDC motor are

shown in Figure.4.3. The $\pi/6$ electrical angle shown in this figure is the advanced phase angle of the current waveforms with respect to the back-EKFs waveforms. Ideally, the conducted current waveforms are in rectangular shapes because only two phases are excited at any instant and the effect of free-wheeling diodes is ignored. The strategy of conduct power MOSFETs, aup, adown, bup, bdown, cups, and cdown, are defined in Figure 4.3. The purpose of using Stateflow® toolbox is to draw the trapezoidal back-EMFs and these six conduct timings.

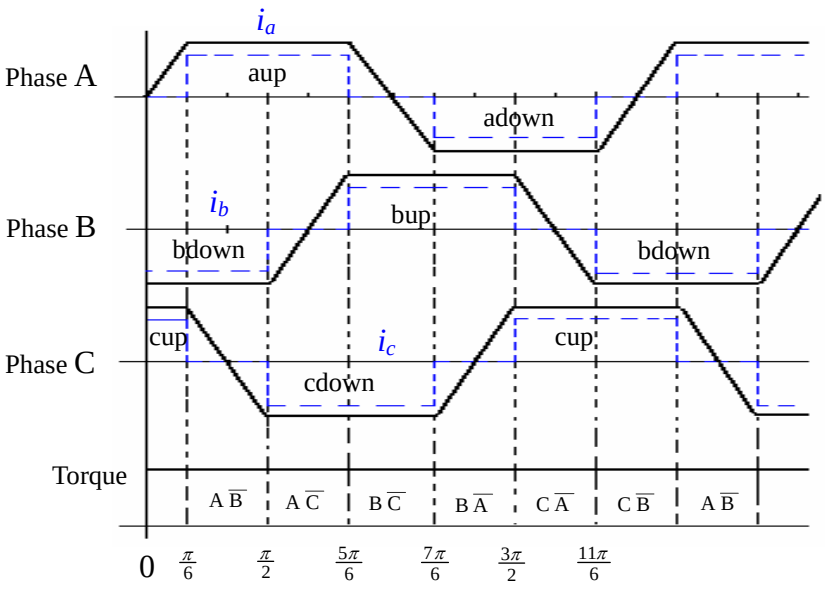

Figure. 4.3 The ideal trapezoidal back-EMFs and torque production in a Y-connected three phase BLDC motor.

In general analysis of the phase voltage, the effect of the free-wheeling diodes is ignored. However, the effect will be taken into highly consideration in this thesis. In principle, the phase current can not be changed suddenly because the inductance exists. Therefore, the segment $A\overline{C}$ switched to the segment $B\overline{C}$ in Figure 4.3 is an

example. The diode will be conducted so that the current of the phase *A* will pass through the diode until the current of the phase *A* decay to zero. The flow chart of this example is shown in Figure 4.4. On these grounds, the complete phase voltages depended on the electrical angle are listed in Table 4.1. Note that the phase voltage is equal to the back-EMF somewhere; the goal is to produce the zero current at that time.

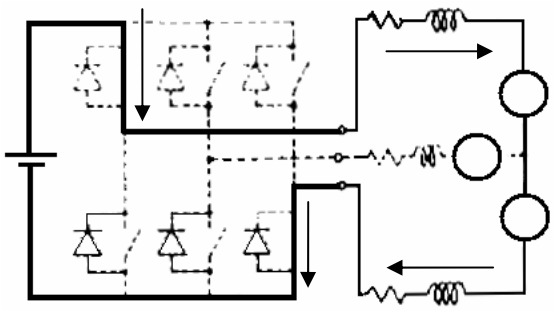

(a)

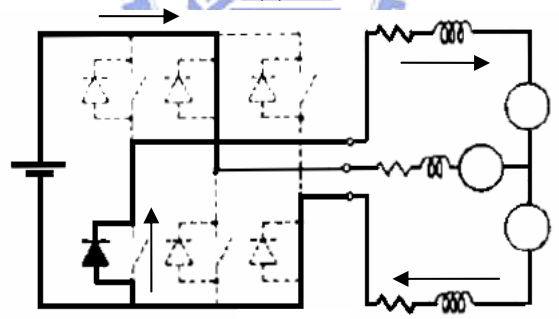

(b)

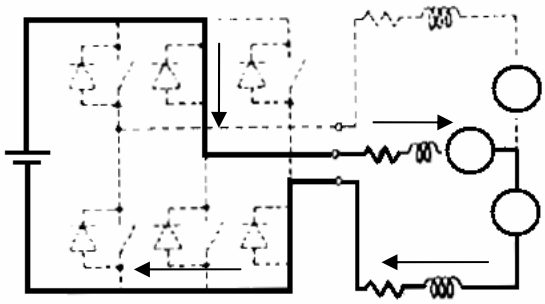

(c)

Figure. 4.4 The flow chart of the commutation sequence. (a) Before commutation; (b) Commutation with two switches and one diode

Table 4.1 The variation of the three phase voltages depended on electrical angle.

segment \ Phase voltage		V_{an}	V_{bn}	V_{cn}
$A\overline{B}$	$I_c>0$	$\frac{2}{3}V_{dc}$	$-\frac{1}{3}V_{dc}$	$-\frac{1}{3}V_{dc}$
	$I_c=0$	$\frac{1}{2}V_{dc}$	$-\frac{1}{2}V_{dc}$	E_c
$A\overline{C}$	$I_b<0$	$\frac{1}{3}V_{dc}$	$\frac{1}{3}V_{dc}$	$-\frac{2}{3}V_{dc}$
	$I_c=0$	$\frac{1}{2}V_{dc}$	E_b	$-\frac{1}{2}V_{dc}$
$B\overline{C}$	$I_a>0$	$-\frac{1}{3}V_{dc}$	$\frac{2}{3}V_{dc}$	$-\frac{1}{3}V_{dc}$
	$I_a=0$	E_a	$\frac{1}{2}V_{dc}$	$-\frac{1}{2}V_{dc}$
$B\overline{A}$	$I_c<0$	$-\frac{2}{3}V_{dc}$	$\frac{1}{3}V_{dc}$	$\frac{1}{3}V_{dc}$
	$I_c=0$	$-\frac{1}{2}V_{dc}$	$\frac{1}{2}V_{dc}$	E_c
$C\overline{A}$	$I_b>0$	$-\frac{1}{3}V_{dc}$	$-\frac{1}{3}V_{dc}$	$\frac{2}{3}V_{dc}$
	$I_b=0$	$-\frac{1}{2}V_{dc}$	E_b	$\frac{1}{2}V_{dc}$
$C\overline{B}$	$I_a<0$	$\frac{1}{3}V_{dc}$	$-\frac{2}{3}V_{dc}$	$\frac{1}{3}V_{dc}$
	$I_a=0$	E_a	$-\frac{1}{2}V_{dc}$	$\frac{1}{2}V_{dc}$

Furthermore, the output torque is proportional to the excited phase current. The idea of the current regulation is to generate the desired torque output by switching six switches of the inverters to control the three phase currents. The hysteresis PWM controller can be accepted to control the rectangular waveforms of the phase currents and its block diagram for a BLDC motor drive is shown in Figure 4.4. Let i^* be a current command, $i^- = i^* - \Delta i$ be a lower limit, $i^+ = i^* + \Delta i$ is an upper limit and i_{fb} be the feedback current, the hysteresis PWM controlled current waveform is shown in Figure 4.5. The switch will be turned OFF when the current rises up to the upper limit

and the current will be fallen due to its time constant. On the contrary, the switch will be turned ON when the current falls down to the lower limit and the current will be charged. Note that only one current controller is requested to control the excited phase current. It is clear that the torque ripple can be decreased by increasing the hysteresis band. However, the inverter switching frequency also increases when the hysteresis band is decreased.

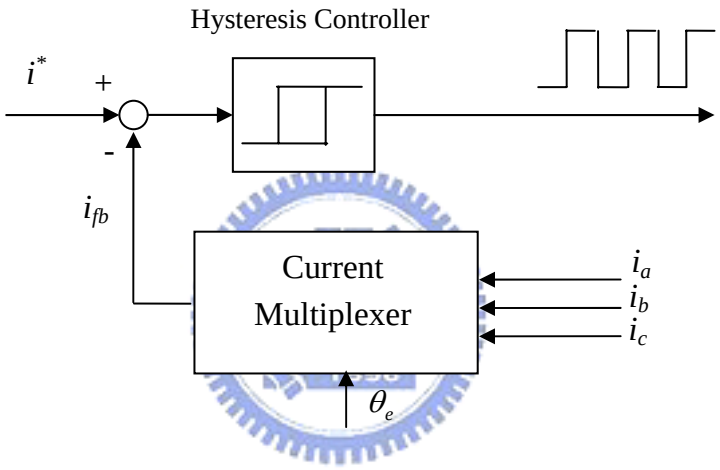

Figure. 4.5 The block diagram of the hysteresis current control.

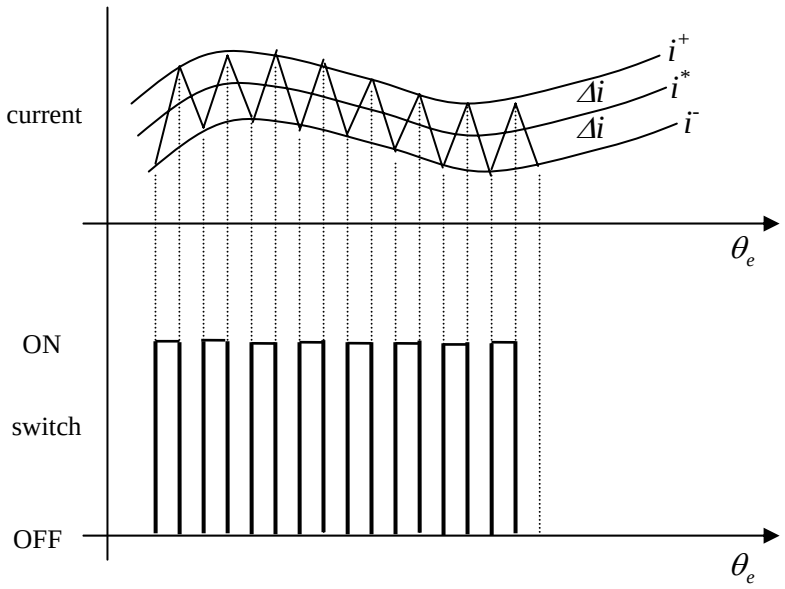

Figure. 4.6 The hysteresis controlled current wavefrom.

The modeling of a BLDC motor will integrate the above components. The speed control with a PID controller and the verified results of the sliding mode estimator will both be shown in Chapter 5.

4.2 Setup a hardware experiment

The hardware experimental plant which is a 3-phase BLDC axial-flux wheel motor is used. It is a low speed and high torque direct-drive motor. The specifications are listed in Table 4.2. The mechanical instrument with a transducer and a brake is set up in Figure 4.6.

Table 4.2 The specification of the BLDC motor.

Pole numbers	16
Slot numbers	48
Operation voltage (volt)	48
Maximum current (Ampere)	15
Maximum unload speed (rpm)	320.9
Back-EMF constant (Volt)	0.18

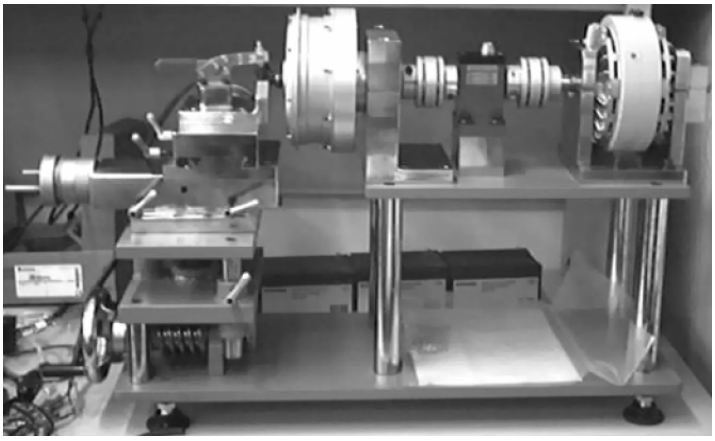

Figure. 4.7 The mechanical instrument of experiment plant.

A complete hardware experiment, PC-based control system, consists of four parts: Pentium®-PC, measurement board, an AD/DA card and a motor driver. The detailed description is shown as follows.

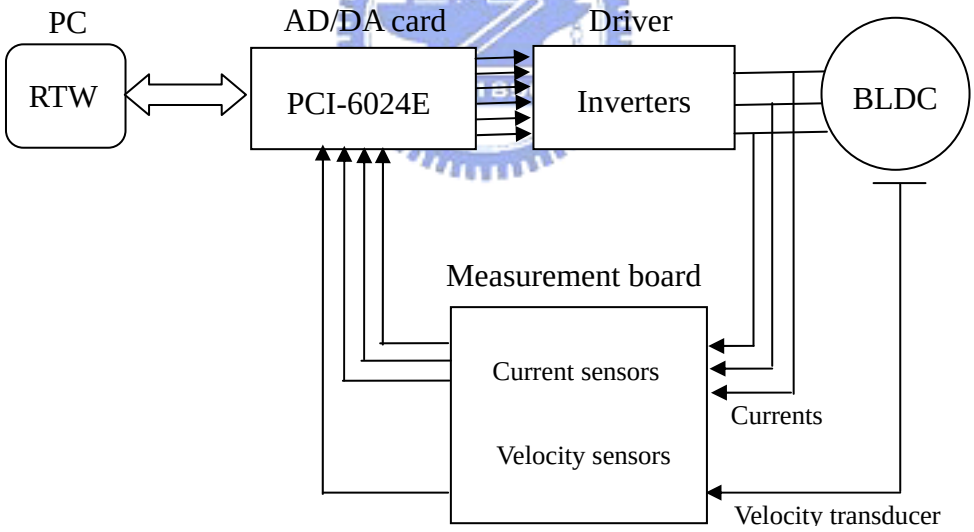

Figure. 4.8 The implementation of a PC-based control system.

Owing to the convenience, visual program design and easy verification, the software in Pentium®-PC uses Real-Time WorkShop® (RTW), a toolbox involved in Matlab®–Simulink®. However, the sampling rate of the RTW is only 1kHz so it can not control in real time. To increase sampling rate, the xPC target can support RTW and it is also a solution to prototyping, testing, and deploying real-time systems that uses a Pentium®-PC. The xPC target is an environment shown in Figure 4.8, using two PC connected by Ethernet line. One is a target PC; the other is a host PC. In addition, xPC target does not require DOS, Windows, Linux or any another operating system on the target PC. The xPC target kernel is booted inside the target PC with a booted disk. After compiling the whole simulation program, the implement file will be loaded into target PC automatically. Consequently, the sampling rate is higher than RTW up to 20kHz.

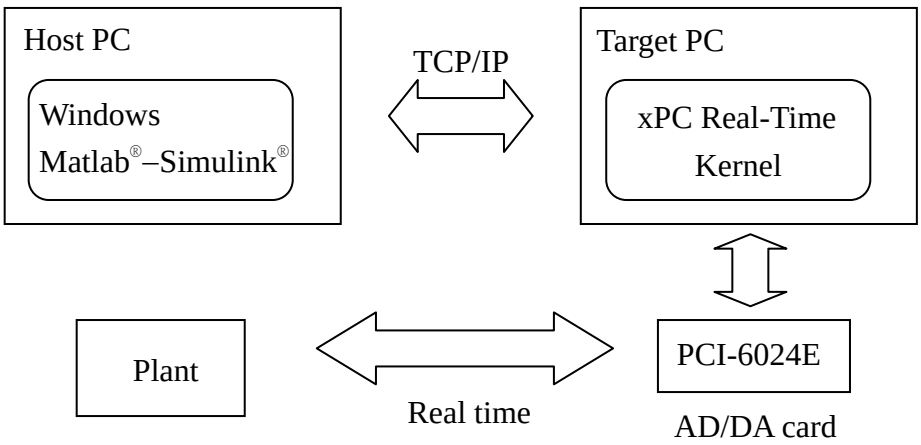

Figure 4.9 The block diagram of the xPC Target environment

The second part of the hardware experiment is an AD/DA card, which is named NI-6024E. The specifications of NI 6024E are PCI-bus, 16 single ended analog inputs at up to 200kSamples per seconds, 2 analog outputs at up to 10kSamples per seconds, 8 digital inputs (outputs) and xpc supportable absolutely.

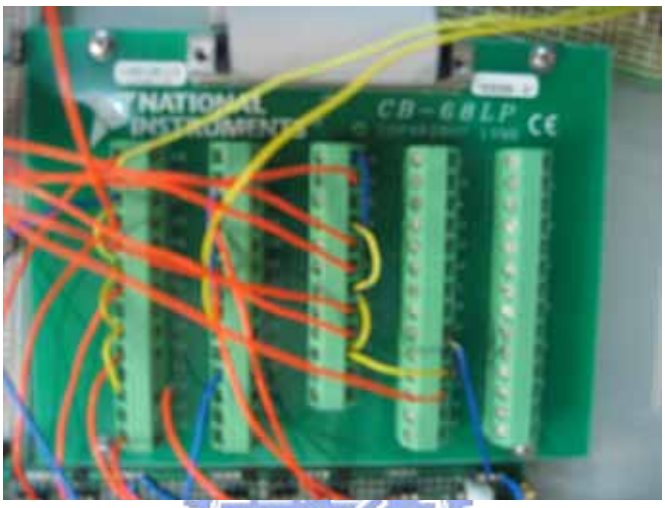

Figure 4.10 The photo of NI-PCI6024E.

Next, the measurement board contains three current sensors and a speed sensor. The LP-25P of the three current sensors is chosen, being able to detect current value up to 25 amperes. The speed sensor is a microcontroller 89C51 that counts pulse-signals from torque transducer, which can output 360 pulses each circle.

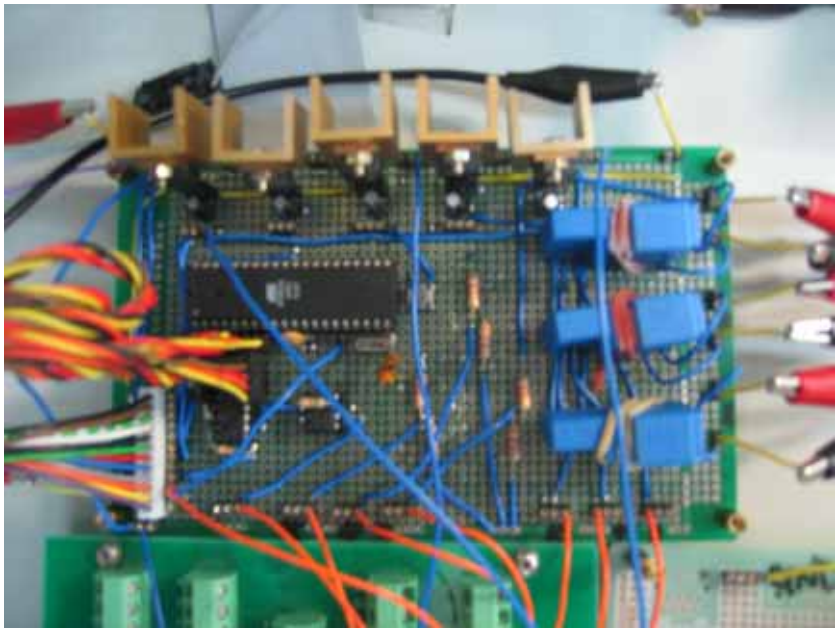

Figure 4.11 The photo of measurement board.

In addition, hardware experiment is designed to verify the use of the estimator. Therefore, the driver that was bought from Crystalyte is used to drive and xPC target aims to measure the terminal currents and voltages when the angular velocity of the motor keeps constant. Next, the estimated angular velocity will be calculated immediately. The experimental results will be shown in the following chapter.